Table 3 Multivariate Cox proportional hazards analysis of factors associated with all-cause and cardiovascular death in hemodialysis patients

	All-cause death			Cardiovascular death		
	Hazard ratio	95% CI	*P*	Hazard ratio	95% CI	*P*
Age (/1 year)	1.11	1.08–1.15	<0.001	1.15	1.10–1.20	<0.001
Hemodialysis duration (/1 year)	0.92	0.87–0.98	0.01	0.94	0.87–1.02	0.14
Diabetes (diabetes vs. no diabetes)	1.26	0.68–2.33	0.46	1.43	0.70–2.90	0.32
Systolic pressure (/1 mmHg)	1.01	0.99–1.03	0.46	1.02	0.98–1.06	0.33
Pulse pressure (/1 mmHg)	1.00	0.96–1.04	0.89	1.01	0.96–1.04	0.81
Lp (a) (/1 mg/dL)	1.00	0.99–1.01	0.79	1.01	1.00–1.06	0.29
ACAI (%)	1.02	0.99–1.04	0.17	1.03	1.00–1.06	0.03

Discussion

Mild renal dysfunction and urinary abnormalities have recently been discovered as strong risk factors for CVD [6]. In HD patients, risk of CVD is 5- to 20-times higher than in the general population, primarily due to early arteriosclerosis [7]. As mentioned previously, vascular calcification has often been reported in HD patients, even at a young age. As indices of vascular calcification in HD patients, aortic arch or common iliac calcification on plain radiographs [8, 9], ACI [3, 4], and EBCT [10] or MDCT [11] have been applied to evaluate coronary artery calcification.

Each of these modalities offers various advantages and disadvantages in terms of convenience, accuracy, and safety. EBCT and MDCT are excellent for quantitative evaluation of coronary artery calcification, but because of the expensive equipment required, are not widely available at many dialysis facilities. Evaluation based on radiographic findings is the most convenient and inexpensive method, and correlations with prognosis have been reported in several reports to date [12, 13]. However, the lack of quantitative evaluation and difficulty of assessing changes over time are still drawbacks.

Plain CT is available even in small and mid-size dialysis centers and is necessary to screen for renal cell carcinoma in HD patients. The advantage is that renal cancer screening and measurement of abdominal aortic calcification can be performed simultaneously. ACAI is a further development of the ACI, which has conventionally been used as an index of abdominal aortic calcification [3, 4]. ACAI provides a more accurate evaluation of calcification in patients with thick calcification, and is also useful to evaluate increases in calcification over time.

The results of our comparison between Group H and Group L showed that systolic blood pressure, pulse pressure, serum calcium concentration, non-HDL cholesterol, Lp (a) concentration and RAS inhibitors, in addition to age, were significantly higher in Group H than in Group L. In 2003, the "Guideline for bone metabolism and disease in chronic kidney disease" by the United States Kidney Disease Outcome Quality Initiative recommended a maximum calcium intake of 1500 mg/day from calcium-containing phosphate binders, widely used as phosphate-binding agents [14]. The goal was prevention of hypercalcemia and excess calcium intake, in light of reports stating that hypercalcemia and excess calcium intake could cause vascular calcification, and that hyperphosphatemia combined with hypercalcemia further increased cardiovascular and mortality risk. Based on these reports, the availability of non-calcium-containing phosphate binders has continued to increase.

Serum levels of calcium, phosphorus and/or intact parathyroid hormone (PTH) levels have been reported to be associated with high levels of CVD morbidity and mortality in patients with end-stage renal disease [15–17]. In this study, serum levels of calcium, phosphate and intact PTH were not associated with cardiovascular mortality. We think the reasons may be as follows. First, when this study was performed, the only available phosphate binder was calcium carbonate, because non-calcium-containing phosphate binders were not available in Japan. Furthermore, the only treatment for secondary hyperparathyroidism was vitamin D agents. Therefore, serum levels of calcium might be high to maintain serum phosphate levels (Group H 9.6 ± 0.4, Group L 9.3 ± 0.4 mg/dL). Furthermore, there were no differences between the two groups with regard to serum levels of intact PTH (Group H 186 ± 83 vs. Group L 196 ± 130 pg/mL; $P = 0.609$). Second, the serum levels of phosphate in the two groups were good control levels and there were no differences between the two groups (Group H 5.2 ± 0.8 vs. Group L 5.3 ± 0.9 mg/dL; $P = 0.857$).

This study evaluated prognostic indicators over a long-term follow-up period of ≥10 years. The most frequent cause of death was cardiovascular death, accounting for 60% of all mortality. Given the long-term evaluation of ≥10 years, age was expected to be a factor with considerable influence. However, on Kaplan–Meier analysis, a high ACAI significantly increased the number of both all-cause deaths and cardiovascular deaths. Univariate Cox hazard analysis showed that age, HD duration, diabetes, systolic blood pressure, pulse pressure, and ACAI were

significant prognostic factors in all-cause death, and that age, HD duration, diabetes, systolic blood pressure, pulse pressure, Lp (a) concentration, and ACAI were significant prognostic factors in cardiovascular death. Ultimately multivariate Cox hazard analysis showed age and HD duration as independent prognostic factors in all-cause deaths. Diabetes, systolic blood pressure, pulse pressure, Lp (a) and ACAI were not significant. But in cardiovascular deaths, age and ACAI were prognostic factors. Our findings suggest that ACAI may be a very useful prognostic indicator for cardiovascular mortality.

Medial calcification is not necessarily associated with lumen stenosis, but because vessel stiffness increases, vascular compliance is decreased [18]. Several mechanisms may explain the association between aortic stiffness and CVD [19]. The arterial stiffness leads to early wave pressure, a decrease of diastolic blood pressure, and a consequent increase of pulse pressure [20]. This increases systolic blood pressure and afterload on the heart, causes left ventricular hypertrophy, and increases myocardial-oxygen demand [21]. In addition, because myocardial blood supply depends largely on pressure throughout diastole and the duration of diastole, the decrease of diastolic blood pressure can compromise coronary perfusion [22]. ACAI as a prognostic factor in cardiovascular death, as demonstrated by our study, may be related to these underlying mechanisms.

We previously published the ACAI method [4]. The ACAI provides a more accurate evaluation of calcification than ACI. However, our study evaluated the relationship between the ACAI measured at one time and future prognosis. In the future, factors leading to serial increases in ACAI, and the influence of these serial increases on prognosis, should be investigated.

Conclusion

Our evaluation of prognosis in 137 HD patients over a period of $\geq$10 years found that the most common cause of mortality was cardiovascular death. In HD patients, ACAI, as measured by abdominal plain CT, was useful as a significant predictive parameter of cardiovascular mortality.

Acknowledgment This work was supported in part by the Grant-in-Aid from the Japanese Society for the Promotion of Science (20590982, 23591222 to T.S.), and by the Public Welfare Science Research Funds (22141101 to T.S.).

References

1. Goodman WG, Goldin J, Kuizon BD, Yoon C, Gales B, Sider D, et al. Coronary-artery calcification in young adults with end-stage renal disease who are undergoing dialysis. N Engl J Med. 2000;18:1478–83.
2. Nakai S, Masakane I, Akiba T, Iseki K, Watanabe Y, Itami N, et al. Overview of regular dialysis treatment in Japan (as of 31 December 2005). Ther Apher Dial. 2007;11:411–41
3. Yukawa S, Sonobe M, Yukawa A, Mimura K, Mune M, Maeda H, et al. Prevention of aortic calcification in patients on hemodialysis by long-term administration of vitamin E. J Nutr Sci Vitam. 1992;38(Suppl):S187–90.
4. Taniwaki H, Ishimura E, Tabata T, Tsujimoto Y, Shioi A, Shoji T, et al. Aortic calcification in haemodialysis patients with diabetes mellitus. Nephrol Dial Transpl. 2005;20(11):2472–8.
5. Ohya M, Otani H, Kimura K, Saika Y, Yukawa S, Shigematsu T, et al. Improved assessment of aortic calcification in Japanese patients undergoing maintenance hemodialysis. Intern Med. 2010;49(19):2071–5.
6. Go AS, Chrtow GM, Fan D, McCulloch CE, Hsu CY. Chronic kidney disease and the risks of death, cardiovascular events, and hospitalization. N Engl J Med. 2004;351:1296–305.
7. Foley R, Parfrey PS, Sarnak MJ. Clinical epidemiology of cardiovascular disease in chronic renal disease. Am J Kidney Dis. 1998;32(Suppl):S112–9.
8. Shigematsu T, Kono T, Satoh K, Yokoyama K, Yoshida T, Hosoya T, et al. Phosphate overload accelerates vascular calcium deposition in end-stage renal disease patients. Nephrol Dial Transpl. 2003;18(Suppl 3):iii86–9.
9. London GM, Guerin AP, Marhais SJ, Metivier F, Pannier B, Adda H. Arterial media calcification in end-stage renal disease: impact on all-cause and cardiovascular mortality. Nephrol Dial Transpl. 2003;18:1731–40.
10. Raggi P, Boulay A, Chasan-Taber S, Amin N, Dillon M, Burke SK, et al. Cardiac calcification in adult hemodialysis patients. A link between end-stage renal disease and cardiovascular disease? J Am Coll Cardiol. 2002;39:695–701.
11. Yokoyama K, Nishioka M, Sakuma T, Yoshida S, Iida R, Yoshida H, et al. Most patients with coronary artery calcification have no coronary artery stenosis and hyperphosphatemia should be important in reevaluating the K/DOQI guideline. Ther Apher Dial. 2006;10:101.
12. Okuno S, Ishimura E, Kitatani K, Fujino Y, Kohno K, Maeno Y, et al. Presence of abdominal aortic calcification is significantly associated with all-cause and cardiovascular mortality in maintenance hemodialysis patients. Am J Kidney Dis. 2007;49(3):417–25.
13. Ogawa T, Ishida H, Akamatsu M, Matsuda N, Fujiu A, Ito K, et al. Progression of aortic arch calcification and all-cause and cardiovascular mortality in chronic hemodialysis patients. Int Urol Nephrol. 2010;42(1):187–94.
14. K/DOQI Workgroup. Clinical practice guideline for bone metabolism and disease in chronic kidney disease. Am J Kidney Dis. 2003;42(3):S62–84.
15. Qunibi WY. Consequences of hyperphosphatemia in patients with end-stage renal disease (ESRD). Kidney Int Suppl. 2004;90:S8–12.
16. Tonelli M, Sacks F, Pfeffer M, et al. Relation between serum phosphate level and cardiovascular event rate in people with coronary disease. Circulation. 2005;112:2627–33.
17. Mathew S, Tustison KS, Sugatani T, et al. The mechanism of phosphorus as a cardiovascular risk factor in CKD. J Am Soc Nephrol. 2008;19:1092–105.
18. Guerin AP, London GM, Marchais SJ, Metivier F. Arterial stiffening and vascular calcification in end-stage renal disease. Nephrol Dial Transpl. 2000;15:1014–21.
19. Mattace-Raso FU, van der Cammen JM, Hofman A, van Popele NM, Bos ML, Schalekamp MADH, et al. Arterial stiffness and risk of coronary heart disease and stroke: the Rotterdam Study. Circulation. 2006;113:657–63.

20. London GM. Large arteries hemodynamics: conduit versus cushioning function. Blood Press Suppl. 1997;2:48–51.
21. Westerhof N, O'Rourke MF. Haemodynamic basis for the development of left ventricular failure in systolic hypertension and for its logical therapy. J Hypertens. 1995;13:943–52.
22. Watanabe H, Ohtsuka S, Kakihana M, Sugishita Y. Coronary circulation in dogs with an experimental decrease in aortic compliance. J Am Coll Cardiol. 1993;21:1497–506.

BRIEF COMMUNICATION www.jasn.org

Fibroblast Expression of an IκB Dominant-Negative Transgene Attenuates Renal Fibrosis

Tsutomu Inoue,* Tsuneo Takenaka,* Matsuhiko Hayashi,† Toshiaki Monkawa,‡ Jun Yoshino,‡ Kouji Shimoda,§ Eric G. Neilson,‖ Hiromichi Suzuki,* and Hirokazu Okada*

*Department of Nephrology, Faculty of Medicine, Saitama Medical University, Saitama, Japan; †Apheresis and Dialysis Center, ‡Department of Internal Medicine, and §Laboratory Animal Center, Keio University School of Medicine, Tokyo, Japan; and ‖Department of Medicine, Vanderbilt University School of Medicine, Nashville, Tennessee

ABSTRACT

It is not clear whether interstitial fibroblasts or tubular epithelial cells are primarily responsible for the profibrotic effects of NF-κB activation during renal fibrogenesis. Here, we crossed mice carrying a conditional IκB dominant-negative transgene (*IκBdN*) with mice transgenic for cell-specific *FSP1.Cre* (FSP1$^+$ fibroblasts) or *γGT.Cre* (proximal tubular epithelia) and challenged all progeny with unilateral ureteral obstruction. We determined NF-κB activation by nuclear localization of phosphorylated p65 (^{P}p65) in renal tissues after 7 days. We observed inhibition of NF-κB activation in interstitial cells and tubular epithelia in obstructed kidneys of *FSP1.Cre;IκBdN* and *γGT.Cre;IκBdN* mice, respectively, compared with *IκBdN* controls ($P < 0.05$). Deposition of extracellular matrix, however, was significantly lower in the obstructed kidneys of *FSP1.Cre;IκBdN* mice but not in *γGT.Cre;IκBdN* mice ($P < 0.05$). In addition, levels of mRNA encoding the profibrotic PAI-1, fibronectin-EIIIA, and type I (α1) procollagen were significantly lower in obstructed kidneys of *FSP1.Cre;IκBdN* mice compared with *γGT.Cre;IκBdN* mice ($P < 0.05$). Taken together, these data support a profibrotic role for fibroblasts, but not proximal tubular epithelial cells, in modulating NF-κB activation during renal fibrogenesis.

J Am Soc Nephrol 21: 2047–2052, 2010. doi: 10.1681/ASN.2010010003

NF-κB regulates a number of downstream genes involved in a variety of cellular functions leading to tissue remodeling.[1] Activation of NF-κB plays a role in various chronic kidney diseases associated with inflammation and fibrosis,[2] and inhibition of NF-κB signaling effectively attenuates renal injury in experimental animals with unilateral ureteral obstruction (UUO),[3] hypertension,[4] subtotal nephrectomy,[5] protein-overload,[6] adriamycin nephropathy,[7] angiotensin II infusion,[8] or FK506 nephropathy.[9] In these previous studies, agents such as pyrrolidine dithiocarbamate, hepatocyte growth factor, parthenolide, or renin-angiotensin system inhibitors were used to inhibit renal NF-κB activation. The specificity of these agents as inhibitors of NF-κB, however, is questionable,[10] and the cells principally providing NF-κB activation *in vivo* are unknown. Systemic administration of inhibitors that disrupt NF-κB activation also impair host immune responses.[11] Clearly, targeted renal cell-specific inhibition of NF-κB would offer a more informative probe.

Renal fibrosis is the hallmark of chronic kidney disease,[12] and UUO in mice is a standard model of short-term renal fibrogenesis.[13] Over a 3-week interval, UUO initiates a rapid decline of renal blood flow and glomerular filtration, which is followed by hydronephrosis, early interstitial infiltrates, and fibrosis.[13] In this model there is a close association between increasing numbers of fibroblasts and tubular epithelial cell loss,[13] which is the principal interest of this study.

When a truncated form of the *IκBα* gene (IκB dominant-negative [*IκBdN*]), which lacks 54 N-terminal amino acids including the phosphorylation sites essential for NF-κB activation, is transfected into tubular epithelial cells by adenovirus vector, renal tubulointerstitial injury from protein overload attenuates in rats.[10] To determine which renal cells contribute functionally important NF-κB activity during renal fibrogenesis after UUO, we generated transgenic mice bearing the *IκBdN* gene separated from a universal CAG promoter by a floxed STOP sequence (Figure 1A) and bred these *IκBdN* mice with other transgenic mice carrying the gene encoding Cre recombinase under the control of cell type-specific promoters.

We previously described a gene en-

Received January 2, 2010. Accepted August 2, 2010.

Published online ahead of print. Publication date available at www.jasn.org.

Correspondence: Dr. Hirokazu Okada, Department of Nephrology, Faculty of Medicine, Saitama Medical University, 38 Morohongo, Moroyama-cho, Irumagun, Saitama 350-0451, Japan. Phone: 81-49-276-1611; Fax: 81-49-295-7338; E-mail: hirookda@saitama-med.ac.jp

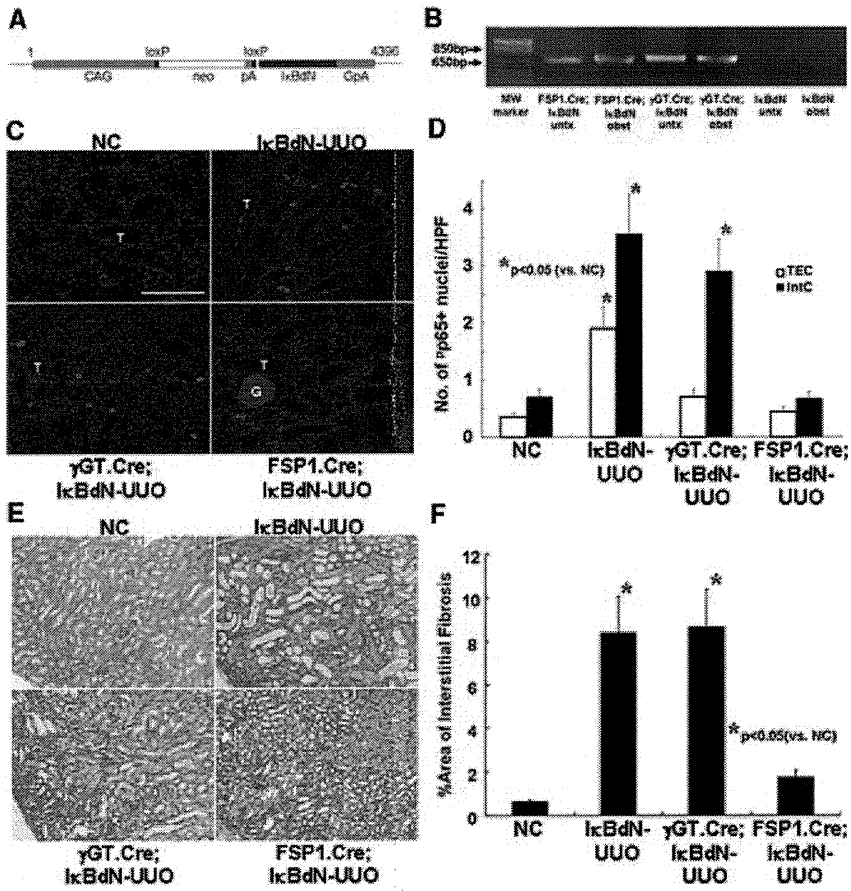

Figure 1. The *IκBdN* gene product blocks activation of the NF-κB pathway in obstructed kidneys. (A) A map of the *IκBdN* transgene. (B) The *IκBdN* gene transcripts were amplified from the total RNA extracts from the kidneys of *FSP1.Cre;IκBdN* and *γGT.Cre;IκBdN* mice but not from those of *IκBdN* mice. (C) In the untreated kidneys of *IκBdN* mice, p65 Ser-276 phosphorylation (^{P}p65 in red) was not found. Numerous nuclei of tubular epithelial cells and fibroblasts were positive for ^{P}p65 in the obstructed kidneys of *IκBdN* mice. The number of ^{P}p65 $^{+}$ nuclei was lower, especially in the tubular epithelial cells, in the obstructed kidneys of *γGT.Cre;IκBdN* mice than those of *IκBdN* mice. In the obstructed kidney of *FSP1.Cre;IκBdN* mice, induction of ^{P}p65 was significantly suppressed compared with that of *IκBdN* mice (objective lens, ×40; bar, 100 μm). (D) Quantification of the number of ^{P}p65^{+} nuclei in the obstructed kidneys by the point-counting method described under Concise Methods. (E) Compared with the untreated kidney, significant ECM deposition was observed in the renal interstitium of *IκBdN* mice with UUO. Significant ECM deposition was also observed in the obstructed kidney of *γGT.Cre;IκBdN* mice. ECM deposition was significantly decreased in the obstructed kidney of *FSP1.Cre;IκBdN* mice compared with that of *IκBdN* mice (Masson's trichrome stain; objective lens, ×10). (F) ECM deposition in the kidneys was quantitatively measured. The data shown in D and F were obtained from six independent mice. T, tubules; G, glomerulus; untx, untreated; obst, obstructed; NC, negative control; TEC, tubular epithelial cells; IntC, interstitial cells; MW, molecular weight.

coding fibroblast-specific protein 1 (*FSP1*),[14] also known as *S100A4*, that is present in fibroblasts producing type I collagen,[15,16] in bone marrow fibrocytes,[17] and in tubular epithelial cells[14,18–21] or endothelial cells[22,23] undergoing transition to fibroblasts.[24] The *FSP1* promoter contains a proximal *cis*-acting enhancer element, *FTS-1*, which broadly functions to engage the larger fibrosis-related transcriptome.[20] *FSP1.Cre* mice have been successfully used to create null alleles in fibroblasts for TGFβ type II receptors,[25] EP4 receptors,[26] and Pten.[27] In our preliminary experiments, crossing transgenic mice expressing Cre recombinase under the control of the *FSP1* promoter (*FSP1.Cre* mice)[25] with mice in which an *EGFP* reporter gene is separated from the universal *CAG* promoter by a floxed STOP sequence (*EGFP* mice)[28] produced conditional progeny whose *FSP1* promoter is active in fibroblasts that costain for enhanced green fluorescent protein (EGFP) and heat shock protein 47, the collagen type I chaperone protein[29] (Supplemental Figure S1, A and B). The number of EGFP^{+} interstitial cells by point counting is significantly increased in obstructed kidneys compared with untreated kidneys from *FSP1.Cre;EGFP* mice (9.2 ± 8.3 and 0.4 ± 0.1 cells/high power field; $P < 0.05$).

We also reported previously that the promoter for γ-glutamyltranspeptidase (*γGT*) driving Cre recombinase only expresses in the cortical tubular epithelium in the kidney of *γGT.Cre* mice,[17] confirmed by others.[30] As expected, *γGT* promoter-driven EGFP^{+} cortical tubular cells were found in the kidneys of *γGT.Cre;EGFP* mice (Supplemental Figure S1A). In those mice stressed by UUO, in confirmation of the previous findings,[17,21] not only cortical tubular epithelium but also solitary cells in the interstitium were positive for EGFP (Supplemental Figure S1A), some of which were also positive for heat shock protein 47 (Supplemental Figure S1B), and some of these latter cells are likely derived by epithelial-mesenchymal transition after ureteral obstruction.

We next crossed *γGT.Cre* or *FSP1.Cre* mice with *IκBdN* mice to generate progeny in which inhibition of NF-κB activation by IκBdN is predicted in cortical tubular epithelial cells or fibroblasts, respectively. This prediction was confirmed by the following results. As shown in Figure 1B, the 712-bp fragment within the *IκBdN* gene transcript[10] could be amplified from untreated and obstructed kidneys of *FSP1.Cre;IκBdN* and *γGT.Cre;IκBdN* mice but not from *IκBdN* controls. These findings suggest that recombination by each cell-specific promoter floxed the *IκBdN* gene driven by

the CAG promoter. The numbers of nuclei positive for phosphorylated p65 Ser-276 (^{P}p65; activated NF-κB)[1] within cortical tubular epithelial cells and fibroblasts in the obstructed kidneys of *γGT.Cre;IκBdN* and *FSP1.Cre;IκBdN* mice, respectively, were significantly ($P < 0.05$) lower than those of *IκBdN* control mice (Figure 1, C and D). The finding that NF-κB activation was attenuated also in tubular epithelial cells from *FSP1.Cre;IκBdN* mice (Figure 1, C and D) suggests that some intermediate epithelia are undergoing epithelial-mesenchymal transition, activating *IκBdN* by early expression of *FSP1*,[17], or perhaps FSP1$^+$ fibroblasts transactivate the NF-κB pathway in tubular epithelial cells by paracrine effects in the obstructed kidney.

It is also of particular interest that deposition of interstitial extracellular matrix (ECM) is significantly ($P < 0.05$) decreased in the *FSP1.Cre;IκBdN* kidneys after UUO but not in the *γGT.Cre;IκBdN* kidneys compared with *IκBdN* controls (Figure 1, E and F). This is because the NF-κB pathway in FSP1$^+$ fibroblasts derived from sources other than cortical tubular epithelium that constitute 64% of whole fibroblasts[17] would still be active in the obstructed kidneys of *γGT.Cre;IκBdN* mice but not in those of *FSP1.Cre;IκBdN* mice, suggesting that the results are consistent with an important role for NF-κB activity in FSP1$^+$ fibroblasts. Additionally, the numbers of F4/80$^+$ macrophages and FSP1$^+$ fibroblasts in the renal interstitium of the *FSP1.Cre;IκBdN* mice after UUO are significantly lower ($P < 0.05$) than those in the *γGT.Cre;IκBdN* and *IκBdN* mice (Figure 2, A through C). All of these findings suggested that NF-κB activation in FSP1$^+$ fibroblasts plays a pivotal role in expanding renal fibrogenesis.

Although expression of chemoattractant genes such as fractalkine (FRK) and osteopontin (OPN) are expectedly decreased in obstructed kidneys from *γGT.Cre;IκBdN* mice, expression of profibrotic transcripts such as plasminogen activator-1 (PAI-1), fibronectin EIIIA (FN-EIIIA), and type I (α1) procollagen (COLI) are increased to the same degrees as those in *IκBdN* controls (Figure 2D). In contrast, in the obstructed kidneys of *FSP1.Cre.IκBdN* mice, expression of all of these profibrotic transcripts was significantly decreased ($P < 0.05$), whereas expression of chemoattractant genes was unchanged compared with those of *IκBdN* mice (Figure 2D). The reason that F4/80$^+$ monocyte infiltration is lower in the obstructed kidney of *FSP1.Cre;IκBdN* mice in spite of a slight increase in transcripts encoding FRK and OPN is unclear. Because F4/80$^+$ macrophages do not express FSP1,[31] *FSP1* promoter-driven expression of *IκBdN* is unlikely in these cells (Figure S1B). An explanation may be that PAI-1 recruits inflammatory cells into the obstructed kidney,[12] or other

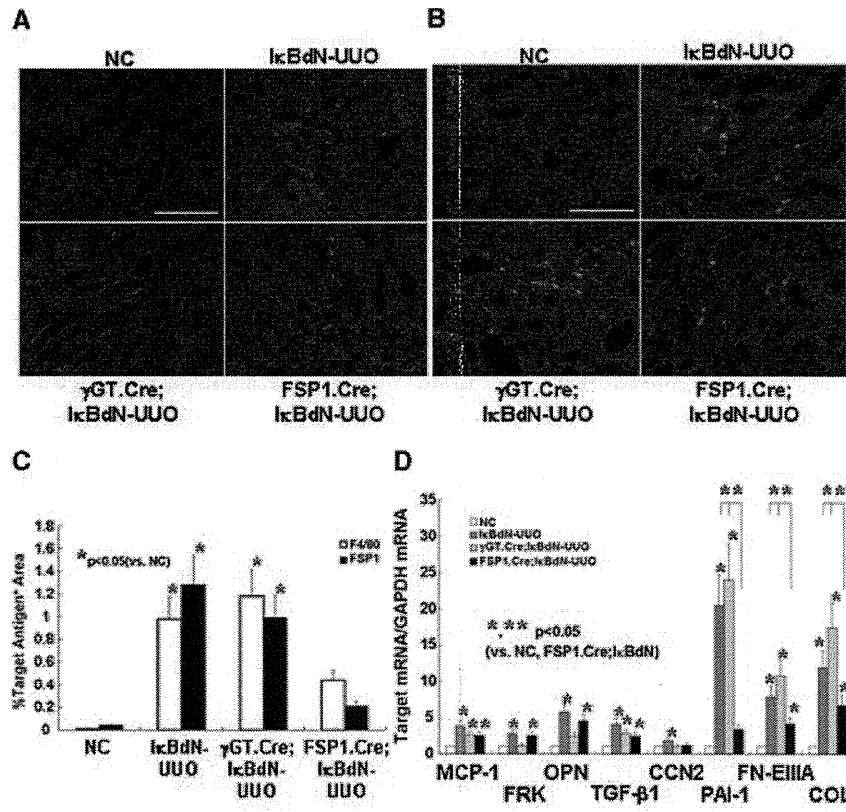

Figure 2. Infiltration of monocytes/fibroblasts and levels of fibrosis-related mRNAs are decreased in the obstructed kidneys of *FSP1.Cre;IκBdN* mice. (A and B) Immunostaining for F4/80$^+$ monocytes (in red) (A) and FSP1$^+$ fibroblasts (in green) (B) in the obstructed kidneys (objective lens, ×40; bar, 100 μm). (C) Quantitative analysis revealed that both the F4/80$^+$ and FSP1$^+$ areas were significantly narrowed in the obstructed kidney of *FSP1Cre.IκBdN* mice, compared with those of *IκBdN* and *γGT.Cre;IκBdN* mice. (D) The mRNA levels of representative inflammatory-related gene, MCP-1, and fibrosis-related gene TGF-β1 were significantly increased in the obstructed kidneys of *IκBdN*, *γGT.Cre;IκBdN*, and *FSP1.Cre;IκBdN* mice. Other inflammatory-related mRNAs such as FRK and OPN were significantly increased in the obstructed kidneys of *IκBdN* mice, which were suppressed in the *γGT.Cre;IκBdN* mice but not in the *FSP1.Cre;IκBdN* mice. In contrast, other fibrosis-related mRNAs such as PAI-1, FN-EIIIA, and COLI were significantly increased in the obstructed kidneys of *IκBdN* and *γGT.Cre;IκBdN* mice, whereas increases in those genes were suppressed in the obstructed kidneys of *FSP1.Cre;IκBdN* mice. In the case of the *CCN2* gene, its mRNA level was increased in the obstructed kidneys of *IκBdN* mice, whereas such increases were suppressed in those of *γGT.Cre;IκBdN* and *FSP1.Cre;IκBdN* mice. The data shown in C and D were obtained from six independent mice. NC, negative control.

pivotal chemoattractant signals[13,32] not tested in this study were suppressed in *FSP1.Cre;IκBdN* mice.

Additionally, it is of interest that the expression of transcripts encoding TGF-β1, a master gene of organ fibrogenesis,[12] is similar in the obstructed kidneys of *IκBdN*, *γGT.Cre;IκBdN*, and *FSP1.Cre;IκBdN* mice despite less fibrogenesis in the obstructed kidneys of *FSP1.Cre;IκBdN* mice (Figure 1, E and F, and Figure 2D). This suggests that FSP1$^+$ fibroblasts are effector cells of TGF-β1 activity in the obstructed kidneys, and the profibrotic actions of TGF-β1 are mediated, at least partially, through the NF-κB pathway in those cells.

We also found consistency in a parallel experiment where treatment with TGF-β1 significantly increased the mRNA levels encoding PAI-1 and FN-EIIIA in cultured renal fibroblasts, which are suppressed by pretreatment with an Iκ kinase inhibitor (Supplemental Figure S2). Although detailed mechanistic links between TGF-β1 signaling to NF-κB activation in renal fibroblasts remain unknown at present, in chondrosarcoma cells, TGF-β1 activates the NF-κB pathway through phosphatidylinositol 3-kinase and Akt.[33] TGF-β1 also synergistically induces NF-κB with TNF-α through protein kinase A-dependent p65 acetylation in human lung epithelial cells.[34] The NF-κB pathway likely plays a profibrotic role not only in renal but also in lung, skin, and intestinal fibroblasts.[35–37]

The fibroblasts involved in renal fibrogenesis in obstructed kidneys likely originate from several sources including interstitial resident fibroblasts,[17,38] bone marrow-derived fibrocytes,[31,17] tubular epithelia,[17] and endothelial cells.[22] *FSP1* promoter-dependent recombination is likely active in all of these sources of fibroblasts. Taking the data from *γGT.Cre;IκBdN* and *FSP1.Cre;IκBdN* mice together suggests that FSP1$^+$ fibroblasts derive from multiple sources and play a profibrotic role in NF-κB-mediated fibrosis in the kidneys. Consistent with this study, we also reported previously that suicide deletion of FSP1$^+$ fibroblasts with a nucleoside analog attenuates renal fibrosis after ureter obstruction.[39] We suggest that a *FSP1* promoter-driven approach will target cells critical for fibrosis-specific therapeutics, and further studies will refine its application to clinical nephrology.

CONCISE METHODS

Transgenic Mice

Three sets of transgenic mice were used, and another was constructed for this study. The *FSP1.Cre* and *γGT.Cre* mice express Cre recombinase under the control of *FSP1* promoter mainly in fibroblasts[25] and that of *γGT* promoter mainly in tubular epithelia,[17] respectively. The *EGFP* reporter mice were a generous gift from Prof. J. Miyazaki (Osaka University).[28] In the *IκBdN* mice, the I*κBdN* gene encoding a nondegraded IκBα that lacks 54 amino acids of the NH_2 terminus of wild-type human IκBα was removed from pBKCMV-IκBdN (a generous gift from Prof. A. Takayanagi, Keio University School of Medicine) by digestion with HindIII, and the overhang ends were blunted with Klenow fragment. The blunted *IκBdN* transgene was then ligated to the SmaI site of the pCALNL5 plasmid (a generous gift from Prof. I. Saito, University of Tokyo),[40] which was separated from the universal CAG promoter by a floxed STOP (neo + pA) sequence (Figure 1A). The construct selected for proper orientation was then linearized using SalI and HindIII, and the purified DNA was injected into B6xSJL zygotes. The resulting progeny were crossed to C57B6 mice and selected by Southern blot and PCR. All of these mice were backcrossed to SJL mice more than six times before experimentation. The Institutional Animal Care and Use Committee at the Saitama Medical University and Keio University School of Medicine approved the transgenic protocols.

DNA was extracted from tail biopsies from *FSP1.Cre*, *γGT.Cre*, *EGFP*, *IκBdN*, *FSP1.Cre;IκBdN*, *γGT.Cre;EGFP*, and *γGT.Cre;IκBdN* mice, and genotyping PCR was performed with an Extract-N-Amp Tissue PCR Kit (XNAT2; Sigma, St. Louis, MO) according to the manufacturer's instructions. The following PCR primers and annealing temperatures were used: *γGT.Cre* and *FSP1.Cre*: 5′-AGGTGTAGAGAAGGCACTTAGC and 3′-CTAATCGCCATCTTCCCAGCAGG, 63°C; *EGFP*: 5′-AGCAAAGGGCGAGGAGCTGTT and 3′-GTAGGTCAGGGTGGTCACGA, 55°C; and *IκBdN*: 5′-GAGGATCGTTTCG-CATGATT and 3′-TATTCGGCAAGCAG-GCATCG, 58°C. Cycle programs were performed in a thermocycler (Icycler; Bio-Rad Japan, Tokyo, Japan). All of the primer reactions were started for 4 minutes at 95°C, followed by 35 cycles of 1 minute at 95°C, 1 minute at the primer's appropriate annealing temperature, and 1 minute at 72°C, finishing with 5 minutes at 72°C. The products were analyzed by electrophoresis in 1% agarose using TAE buffer.

In Vivo Experiments

Six male, 5- to 6-week-old mice from each transgenic line, *γGT.Cre;IκBdN*, *FSP1.Cre;IκBdN*, and *IκBdN*, were used to generate fibrosis in the UUO model. Manipulation for ureter ligation was reported in detail previously.[17] The mice were sacrificed 7 days after ureteral ligation, and obstructed kidney tissues were sampled for RNA extraction and paraformaldehyde fixation for paraffin blocks. *IκBdN* mice with ureteral ligation and sham manipulation ($n = 6$) were used as positive and the negative controls, respectively.

Microscopic Immunohistochemistry

Sections (4 μm) cut from paraffin-embedded kidneys were processed for Masson's trichrome staining. Interstitial fibrosis was quantitatively determined with Mac SCOPE software (version 2.5; Mitani Corp., Fukui, Japan) in 10 high-power (×200) cortical fields, and the interstitial fibrosis indices were expressed as the mean percentage area in blue per one cortical field in Masson's trichrome-stained sections.[41] For immunohistochemistry, the antibodies against EGFP (ab13970; Abcam, Cambridge, UK), ^{P}p65 (3037; Cell Signaling Technology, Boston, MA), mouse monocytes (F4/80; AbD Serotec, Oxford, UK), and fibroblasts (FSP1)[14] were diluted (1:400) into 1% BSA in PBS as the blocking buffer and then applied on the sections for 8 hours. Except for EGFP, the signals were amplified using TSA™ kit (Molecular Probe/Invitrogen, Carlsbad, CA) and labeled by Alexa Fluor 555 (Molecular Probe). Alexa Fluor 488-labeled secondary antibody was used after anti-EGFP antibody according to a conventional indirect method. Negative control sections were

treated as described above, but the primary antibody was omitted. YO-PRO-1 (Molecular Probe) or TO-PRO-3 (Molecular Probe) was used to detect the nuclei. A confocal laser scanning microscopy (FV1000; Olympus, Tokyo, Japan) was used for data acquisition. The number of $^{P}p65^{+}$ nuclei were counted in 10 microscopic fields using a 40× objective lens, and its indices were expressed as the mean number per one field. The numbers of stained cells for anti-F4/80 and anti-FSP1 were quantitatively assessed as described above.

Reverse Transcriptase (RT)-PCR

Total RNA was extracted from the homogenates of kidney tissues with TRIzol™ (Life Technologies BRL, Grand Island, NY) according to the manufacturer's instructions. All of the RNA samples were pretreated with the RNase-free DNase I (Qiagen, Basel, Switzerland). cDNA was synthesized with a kit (Ready-To-Go T-Primed First-Strand Kit; GE Healthcare, Buckinghamshire, UK). The cDNA was amplified by PCR with the use of primers for *IκBdN* (forward, 5′-CTCCAGCAGACTCCACTCCACT-3′, and reverse, 5′-ACACCAGCCACCACCTTCTGAT-3′), yielding a 712-bp fragment. Cycle programs were started with 4 minutes at 95°C, followed by 35 cycles of 1 minute at 95°C, 1.5 minutes at 60°C, and 1.5 minutes at 72°C, finishing with 5 minutes at 72°C.

Real-Time Quantitative RT-PCR (qPCR)

We performed qPCR as described previously.[41] In brief, a real-time quantitative one-step RT-PCR assay was performed to quantify mRNA levels using QuantiTect SYBR Green RT-PCR (Qiagen) and an Mx3000P QPCR system (Stratagene, La Jolla, CA). The primers used for qPCR were as follows: MCP-1 primer: forward, 5′-CTCTCTTCCTCCACCACCAT-3′, and reverse, 5′-ACTGCATCTGGCTGAGCCA-3′; FRK primer: forward, 5′-CGCGTTCTTCCATTTGTGTA-3′, and reverse, 5′-CATGATTTCGCATTTCGTCA-3′; OPN primer: forward, 5′-CCCTTTCCGTTGTTGTCCTG-3′, and reverse, 5′-CCCTCGATGTCATCCCTGTT-3′; TGF-β1 primer: forward, 5′-CAGTGGCTGAACCAAGGAGAC-3′, and reverse, 5′-ATCCCGTTGATTTCCACGTG-3′; CCN2 primer: forward, 5′-GTGGAATATTGCCGGTGCA-3′, and reverse, 5′-CCATTGAAGCATCTTGGTTCG-3′; PAI-1 primer: forward, 5′-AGGATCGAGGTAAACGAGAGC-3′, and reverse, 5′-GCGGGCTGAGATGACAAA-3′; FN-EIIIA primer: forward, 5′-ATCCGGGAGCTTTTCCCTG-3′, and reverse, 5′-TGCAAGGCAACCACACTGAC-3′; COLI primer: forward 5′-TGTAAACTCCCTCCACCCCA-3′, and reverse, 5′-TCGTCTGTTTCCAGGGTTGG-3′; and glyceraldehyde-3-phosphate dehydrogenase primer: forward, 5′-TGCAGTGGCAAAGTGGAGATT-3′, and reverse, 5′-TTGAATTTGCCGTGAGTGGA-3′. All of these oligodeoxynucleotides were designed by using Primer Express software (Perkin Elmer, Foster City, CA). Preliminary RT-PCR experiments in which these primer sets were used yielded appropriately sized, single products.

Statistical Analysis

The values are presented as the means ± SEM. The statistical differences between groups were evaluated by ANOVA, followed by a Bonferroni/Dunnett's test; significant P values were ≤ 0.05.

ACKNOWLEDGMENTS

The authors thank M. Funabashi for her technical assistance. This research was supported in part by grants from Asubio Pharma Co. Ltd., the Ministry of Education, Culture, Sports, Science and Technology (Japan), and the Ministry of Health, Labour and Welfare (Japan). EGN was supported by National Institutes of Health Grant DK-46282.

DISCLOSURES

None.

REFERENCES

1. Hayden MS, Ghosh S: Shared principles in NF-kB signaling. *Cell* 132: 344–362, 2008
2. Guijarro C, Egido J: Transcription factor-kappa B (NF-kappa B) and renal disease. *Kidney Int* 59: 415–424, 2001
3. Giannopoulou M, Dai C, Tan X, Wen X, Michalopoulos GK, Liu Y: Hepatocyte growth factor exerts its anti-infammatory action by disrupting nuclear factor-kB signaling. *Am J Pathol* 173: 30–41, 2008
4. Rodriguez-Iturbe B, Ferrebuz A, Vanegas V, Quiroz Y, Mezzano SA, Vaziri ND: Early and sustained inhibition of nuclear factor-kappaB prevents hypertension in spontaneously hypertensive rats. *J Pharmacol Exp Ther* 315: 51–57, 2005
5. Fujihara CK, Antunes GR, Mattar AL, Malheiros, DMAC, Vieira JM, Zatz R: Chronic inhibition of nuclear factor-kB attenutaes renal injury in the 5/6 renal ablation model. *Am J Physiol Renal Physiol* 292: F92–F99, 2007
6. Gomez-Garre D, Largo R, Tejera N, Fortes J, Manzarbeitia F, Egido J: Activation of NF-kB in tubular epithelial cells of rats with intense proteinuria. *Hypertension* 37: 1171–1178, 2001
7. Rangan GK, Wang Y, Tay YC, Harris DC: Inhibition of nuclear factor-kB activation reduces cortical tubulointerstitial injury in proteinuric rats. *Kidney Int* 56: 118–134, 1999
8. Ozawa Y, Kobori H: Crucial role of Rho-nuclear factor-kB axis in angiotensin II-induced renal injury. *Am J Physiol Renal Physiol* 293: F100–F109, 2007
9. Tamada S, Nakatani T, Asai T, Tashiro K, Komiya T, Sumi T, Okamura M, Kim S, Iwao H, Kishimoto T, Yamanaka S, Miura K: Inhibition of nuclear factor-kB activation by pyrrolidine dithiocarbamate prevents chronic FK506 nephropathy. *Kidney Int* 63: 306–314, 2003
10. Takase O, Hirahashi J, Takayanagi A, Chkaraishi A, Marumo T, Ozawa Y, Hayashi M, Shimizu N, Saruta T: Gene transfer of truncated IkBa prevents tubulointerstitial injury. *Kidney Int* 63: 501–513, 2003
11. Ouaaz F, Li M, Beg AA: A critical role for the RelA subunit of nuclear factor kB in regulation of multiple immune-response genes and in Fas-induced cell death. *J Exp Med* 189: 999–1004, 1999
12. Okada H, Kalluri R: Cellular and molecular pathways that lead to progression and regression of renal fibrogenesis. *Curr Mol Med* 5: 467–474, 2005
13. Chevalier RL, Forbes MS, Thronhill BA: Ureteral obstruction as a model of renal interstitial fibrosis and obstructive nephropathy. *Kidney Int* 75: 1145–1152, 2009
14. Strutz F, Okada H, Lo CW, Danoff TM, Carone RL, Tomaszewski JE, Neilson EG: Identification and characterization of a fibroblast marker: FSP1. *J Cell Biol* 130: 393–405, 1995
15. Okada H, Danoff TM, Kalluri R, Neilson EG: Early role of Fsp1 in epithelial-mesenchymal transformation. *Am J Physiol* 273: F563–F574, 1997
16. Lawson WE, Polosukhin VV, Zoia O, Stathopoulos GT, Han W, Plieth D, Loyd JE, Neilson EG, Blackwell TS: Characterization of fibroblast-specific protein 1 in pulmonary fibrosis. *Am J Respir Crit Care Med* 171: 899–907, 2005
17. Iwano M, Plieth D, Danoff TM, Xue C, Okada H, Neilson EG: Evidence that fibroblasts de-

rive from epithelium during tissue fibrosis. *J Clin Invest* 110: 341–350, 2002
18. Kie JH, Kapturczak MH, Traylor A, Agarwal A, Hill-Kapturczak N: Heme oxygenase-1 deficiency promotes epithelial-mesenchymal transition and renal fibrosis. *J Am Soc Nephrol* 19: 1681–1691, 2008
19. Kim J, Seok YM, Jung KJ, Park KM: Reactive oxygen species/oxidative stress contributes to progression of kidney fibrosis following transient ischemic injury in mice. *Am J Physiol Renal Physiol* 297: F461–F470, 2009
20. Venkov CD, Link AJ, Jennings JL, Plieth D, Inoue T, Nagai K, Xu C, Dimitrova YN, Rauscher III, FJ, Neilson EG: A proximal activator of transcription in epithelial-mesenchymal transition. *J Clin Invest* 117: 482–491, 2007
21. Higgins DF, Kimura K, Bernhardt WM, Shrimanker N, Akai Y, Hohenstein B, Saito Y, Johnson RS, Kretzler M, Cohen CD, Eckardt KU, Iwano M, Haase VH: Hypoxia promotes fibrogenesis in vivo via HIF-1 stimulation of epithelial-to-mesenchymal transition. *J Clin Invest* 117: 3810–3820, 2007
22. Zeisberg EM, Potenta SE, Sugimoto H, Zeisberg M, Kalluri R: Fibroblasts in kidney fibrosis emerge via endothelial-mesenchymal transition. *J Am Soc Nephrol* 19: 2282–2287, 2008
23. Zeisberg EM, Tarnavski O, Zeisberg M, Dorfman AL, McMullen JR, Gustafsson E, Chandraker A, Yuan X, Pu WT, Roberts AB, Neilson EG, Sayegh MH, Izumo S, Kalluri R: Endothelial-to-mesenchymal transition contributes to cardiac fibrosis. *Nat Med* 13: 952–961, 2007
24. Liu Y: New insights into epithelial-mesenchymal transition in kidney fibrosis. *J Am Soc Nephrol* 21: 212–222, 2010
25. Bhowmick NA, Chytil A, Plieth D, Gorska AE, Dumont N, Shappell S, Washington MK, Neilson EG, Moses HL: TGF-beta signaling in fibroblasts modulates the oncogenic potential of adjacent epithelia. *Science* 303: 848–851, 2004
26. Tsutsumi R, Xie C, Wei X, Zhang M, Zhang X, Flick LM, Schwarz EM, O'Keefe RJ: PGE2 signaling through the EP4 receptor on fibroblasts upregulates RANKL and stimulates osteolysis. *J Bone Miner Res* 24: 1753–1762, 2009
27. Trimboli AJ, Cantemir-Stone CZ, Li F, Wallace JA, Merchant A, Creasap N, Thompson JC, Caserta E, Wang H, Chong JL, Naidu S, Wei G, Sharma SM, Stephens JA, Fernandez SA, Gurcan MN, Weinstein MB, Barsky SH, Yee L, Rosol TJ, Stromberg PC, Robinson ML, Pepin F, Hallett M, Park M, Ostrowski MC, Leone G: Pten in stromal fibroblasts suppresses mammary epithelial tumours. *Nature* 461: 1084–1091, 2009
28. Kawamoto S, Niwa H, Tashiro F, Sano S, Kondoh G, Takeda J, Tabayashi K, Miyazaki J: A novel reporter mouse strain that expresses enhanced green fluorescent protein upon Cre-mediated recombination. *FEBS Lett* 470: 263–268, 2000
29. Okada H, Ban S, Nagao S, Takahashi H, Suzuki H, Neilson EG: Progressive renal fibrosis in murine polycystic kidney disease: an immunohistochemical observation. *Kidney Int* 58: 587–597, 2000
30. Starremans PG, Li X, Finnerty PE, Guo L, Takakura A, Neilson EG, Zhou J: A mouse model for polycystic kidney disease through a somatic in-frame deletion in the 5′ end of Pkd1. *Kidney Int* 73: 1394–1405, 2008
31. Inoue T, Plieth D, Venkov CD, Xu C, Neilson EG: Antibodies against macrophages that overlap in specificity with fibroblasts. *Kidney Int* 67: 2488–2493, 2005
32. Vielhauer V, Anders HJ, Mack M, Cihak J, Strutz F, Stangassinger M, Luckow B, Groene HJ, Schlondorff D: Obstructive nephropathy in the mouse: Progressive fibrosis correlates with tubulointerstitial chemokine expression and accumulation of CC chemokine receptor 2- and 5-positive leukocytes. *J Am Soc Nephrol* 12: 1173–1187, 2001
33. Yeh YY, Chiao CC, Kuo WY, Hsiao YC, Chen YJ, Wei YY, Lai TH, Fong YC, Tang CH: TGF-b1 increases motililty and aVb3 integrin up-regulation via PI3K, Akt and NF-kB-dependent pathway in human chondrosarcoma cells. *Biochem Pharmocol* 75: 1292–1301, 2008
34. Ishinaga H, Jono H, Lim JH, Komatsu K, Xu X, Lee J, Woo CH, Xu H, Feng XH, Chen LF, Yan C, Li JD: Synergistic induction of nuclear factor-kB by transforming growth factor-b and tumour necrosis factor-a is mediated by protein kinase A-dependent RelA acetylation. *Biochem J* 417: 583–591, 2009
35. Chetty A, Cao GJ, Nielsen HC: Insulin-like growth factor-I signaling mechanisms, type I collagen and alpha smooth muscle actin in human fetal lung fibroblasts. *Pediatr Res* 60: 389–394, 2006
36. Messadi DV, Doung HS, Zhang Q, Kelly AP, Tuan TL, Reichenberger E, Le AD: Activation of NFkB signal pathways in keloid fibroblasts. *Arch Dermatol Res* 296: 125–133, 2004
37. Theiss AL, Simmons JG, Jobin C, Lund PK: Tumor necrosis factor (TNF) α increases collagen accumulation and proliferation in intestinal myofibroblasts via TNF receptor 2. *J Biol Chem* 280: 36099–36109, 2005
38. Lin SL, Kisseleva T, Brenner DA, Duffield JS: Pericytes and perivascular fibroblasts are the primary source of collagen-producing cells in obstructive fibrosis of the kidney. *Am J Pathol* 173: 1617–1627, 2008
39. Iwano M, Fischer A, Okada H, Pleith D, Xue C, Danoff T, Neilson E: Conditional abatement of tissue fibrosis using nucleotide analogs to corrupt DNA replication selectively in transgenic fibroblasts. *Mol Ther* 3: 149–159, 2001
40. Kanegae Y, Takamori K, Sato Y, Lee G, Nakai M, Saito I: Efficient gene activation on mammalian cell chromosomes using recombinant adenovirus producing Cre recombinase. *Gene* 181: 207–212, 1996
41. Okada H, Inoue T, Kikuta T, Watabe T, Kanno Y, Ban S, Sugaya T, Horiuchi M, Suzuki H: A possible anti-inflammatory role of angiotensin II type 2 recerptor in immune-mediated glomerulonephritis during type 1 receptor blockade. *Am J Pathol* 169: 1577–1589, 2006

Supplemental information for this article is available online at http://www.jasn.org/.